scientific reports

Check for updates

OPEN

Magnamosis improves the healing of gastrojejunal anastomosis and down-regulates TGF-β1 and HIF-1α in rats

Tianren Wang[1], Yunhao Li[2], Chenao Yu[1], Xinru Lv[3], Yuxuan Weng[3], Zhixuan Zhang[4], Haozhen Xu[3], Runjia Liang[3], Mengyue Wang[3], Zhenzhen Weng[3], Cheng Zhang[3], Yi Lv[5]✉ & Yong Zhang[1]✉

This study elucidated the unique pathological features of tissue healing by magnamosis and revealed the changes in landmark molecule expression levels related to collagen synthesis and tissue hypoxia. Forty-eight male Sprague–Dawley rats were divided into the magnamosis and suture anastomosis groups, and gastrojejunal anastomosis surgery was performed. Rats were dissected at 6, 24, and 48 h and 5, 6, 8, 10, and 12 days postoperatively. Hematoxylin, eosin, and Masson's trichrome staining were used to evaluate granulation tissue proliferation and collagen synthesis density at the anastomosis site. Immunohistochemistry was used to measure TGF-β1 and HIF-1α expression levels. Magnamosis significantly shortened the operation time, resulting in weaker postoperative abdominal adhesions ($P < 0.0001$). Histopathological results showed a significantly lower granulation area in the magnamosis group than in the suture anastomosis group ($P = 0.0388$), with no significant difference in the density of collagen synthesis ($P = 0.3631$). Immunohistochemistry results indicated that the magnamosis group had significantly lower proportions of TGF-β1-positive cells at 24 ($P = 0.0052$) and 48 h ($P = 0.0385$) postoperatively and HIF-1α-positive cells at 24 ($P = 0.0402$) and 48 h postoperatively ($P = 0.0005$). In a rat model of gastrojejunal anastomosis, magnamosis leads to improved tissue healing at the gastrojejunal anastomosis, associated with downregulated expression levels of TGF-β1 and HIF-1α.

Gastrointestinal tissue healing can be divided into three stages: inflammation response, proliferation, and remodeling stages[1]. Fibroblast activation, collagen synthesis, and maturation play crucial roles in the healing of anastomotic site. Smooth muscle cells and fibroblasts, which are the primary cellular components of granulation tissue, participate in collagen synthesis within gastrointestinal tissues[2,3]. Fibroblasts are responsible for generating and reshaping the extracellular matrix, making them essential for tissue repair after injury and the formation of new tissue[4]. Transforming growth factor-β1 (TGF-β1) plays a key role in mediating fibroblast synthesis of collagen fibers[5], promoting the deposition of extracellular matrix at the anastomotic site, and represents one of the fundamental physiological changes in establishing robust tissue healing[6].

Tissue hypoxia occurs in the microenvironment during healing of the anastomotic site. The key molecule for cellular hypoxia sensing and stress response is hypoxia-inducible factor 1 (HIF-1). The α subunit of HIF-1 is sensitive to hypoxic stress, and under normoxic conditions, it undergoes ubiquitination and proteasomal degradation[7]. In addition, HIF-1α can regulate the expression of numerous downstream genes, including TGF-β1[8], influencing adaptive regulation of processes such as collagen synthesis in response to hypoxic stress.

Poor healing at the anastomotic site is a significant complication of gastrointestinal surgery and has a substantial impact on tumor prognosis, patient quality of life, and healthcare economics[9]. The magnamosis technology is used to create an anastomotic pathway through mechanical compression of tissues using the attractive force

[1]Department of Thoracic Surgery, The First Affiliated Hospital of Xi'an Jiaotong University, Xi'an 710067, China. [2]Department of Geriatric Surgery, The Second Affiliated Hospital of Xi'an Jiaotong University, Xi'an 710067, China. [3]Xi'an Jiaotong University Medical Science Center, Xi'an 710067, China. [4]Department of Thoracic Surgery, Peking University People's Hospital, Beijing 100044, China. [5]Department of Hepatobiliary Surgery, The First Affiliated Hospital of Xi'an Jiaotong University, Xi'an 710067, China. ✉email: luyi169@126.com; zhangyongyang05@163.com

between magnets[10,11]. This concept was introduced by Harrison in 2008 and has been well-validated for its effectiveness and safety in experimental porcine jejunal magnetic anastomosis[12]. It has been applied in various surgical fields, including endoscopic gastrojejunostomy, duodenocolonic magnetic anastomosis[10,13], and hybrid NOTES colorectal anastomosis[14], becoming the third preferred method of anastomosis following suture and staple anastomosis[15,16]. Compared with suture anastomosis, magnamosis offers advantages[11,17] such as simplifying the surgical process, increasing anastomosis speed, improving surgical efficiency, reducing the occurrence of complications like anastomotic fistulas and stenosis, and minimizing inflammatory reactions due to the absence of foreign material residue at the anastomotic site.

However, research on the mechanisms of tissue healing at the anastomotic site following gastrojejunal magnamosis remains lacking. Therefore, this study aimed to elucidate the unique pathological features of tissue healing by magnamosis and reveal changes in the expression level of landmark molecules related to collagen synthesis and tissue hypoxia.

Results

Magnamosis shortens the operation time of gastrojejunal anastomosis

The surgical procedure time in the gastrointestinal anastomosis group was significantly shorter than in the sutured anastomosis group. The average time required to establish magnamosis was 8.08 min, whereas that required for sutured anastomosis was 21.87 min (Fig. 1A).

Safety of magnamosis surgery

The postoperative survival of the rats was favorable, with no unexpected deaths or serious adverse events related to the surgery. A decrease in body weight was observed on the first day after surgery; however, this started to increase on the second day. The average postoperative body weight was 250.90 ± 24.49 g in the magnamosis group and 252.20 ± 17.63 g in the suture anastomosis group, with no significant difference between the groups ($P = 0.8835$) (Fig. 1B,C). Postoperative radiography indicated that displacement of the magnets occurred on the 4th–5th day after surgery in both groups (Fig. 2A–C).

Abdominal adhesion of rats improves after magnamosis

The evaluation of abdominal adhesion in rats during the anatomical examination is shown in Fig. 3A and Table 1. The results indicated that rats in the magnamosis group had only mild, easily separable adhesions at the anastomotic site or no adhesions at all. These were mostly observed in the posterior wall of the anastomosis and omentum (Fig. 3B–D). In contrast, compared with the magnamosis group, the suture anastomosis group had more pronounced adhesions, primarily involving the liver and anterior wall of the stomach, often accompanied by mild dilation of the intestinal tract or anastomotic site.

Healing of the magnamosis tissue is smoother, and the proliferation of granulation tissue is weakened on microscopic observation

Results of the anastomotic tissue section staining showed that at 6 h postoperatively, the magnamosis group exhibited evident tissue compression, but the anastomosis had not yet formed. The directly compressed tissue was notably compressed, with the edge of the compressed area being the actual site of adhesive healing. The tissue layers were clear and distinct. In contrast, the suture anastomosis immediately established a patent anastomosis, but the tissue layers were disrupted owing to the cutting injury.

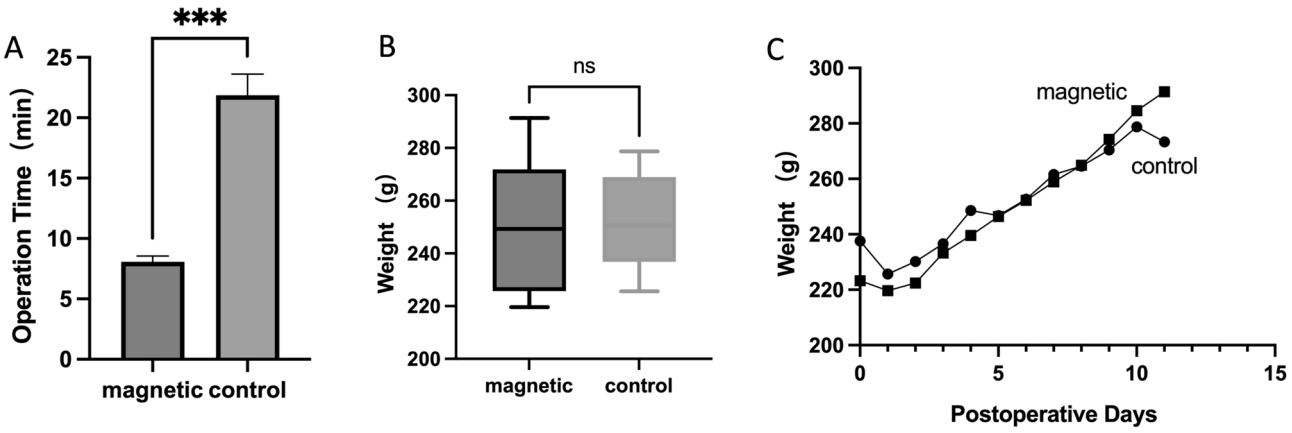

Fig. 1. Postoperative evaluation of gastrojejunal anastomosis in rats. (**A**) Duration of surgical procedures. The establishment of anastomosis in the magnamosis group took significantly less time than that in the control group (***$p < 0.001$). (**B**) Postoperative weight (mean ± SD) showed no statistical difference between the magnamosis and suture anastomosis groups, two-sample independent *t*-test (ns, not significant). (**C**) The line graph showed changes in postoperative weight. Both groups of animals exhibited a decrease in weight only on the first postoperative day, followed by recovery.

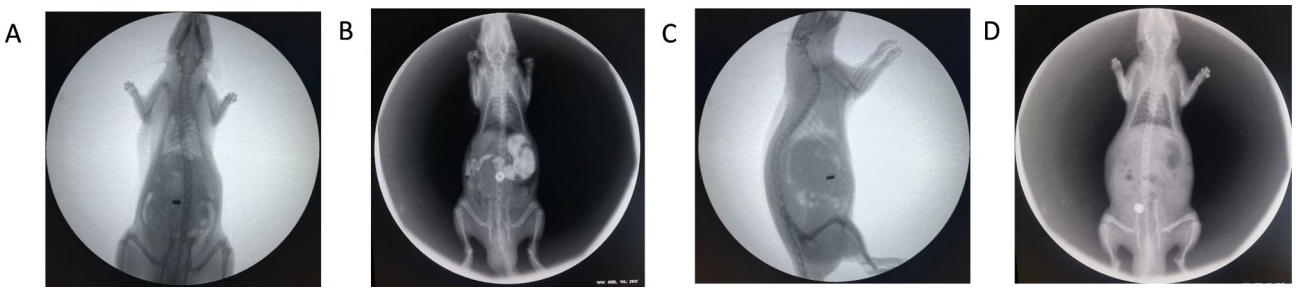

Fig. 2. X-ray and gastrointestinal radiography were taken postoperatively to observe the position of the magnetic ring. (**A**) Lateral and anteroposterior X-ray images showed the position of the magnet rings in the magnamosis group postoperatively. (**B**) X-ray fluoroscopy on postoperative day 1 in the magnamosis group demonstrated the patency of the gastrojejunal tract with the distal stomach and duodenum patent, while the gastric-jejunal anastomosis was not yet patent. (**C**) The magnet ring displacement observed on X-ray fluoroscopy in the magnamosis group occurred at 4th day postoperatively.

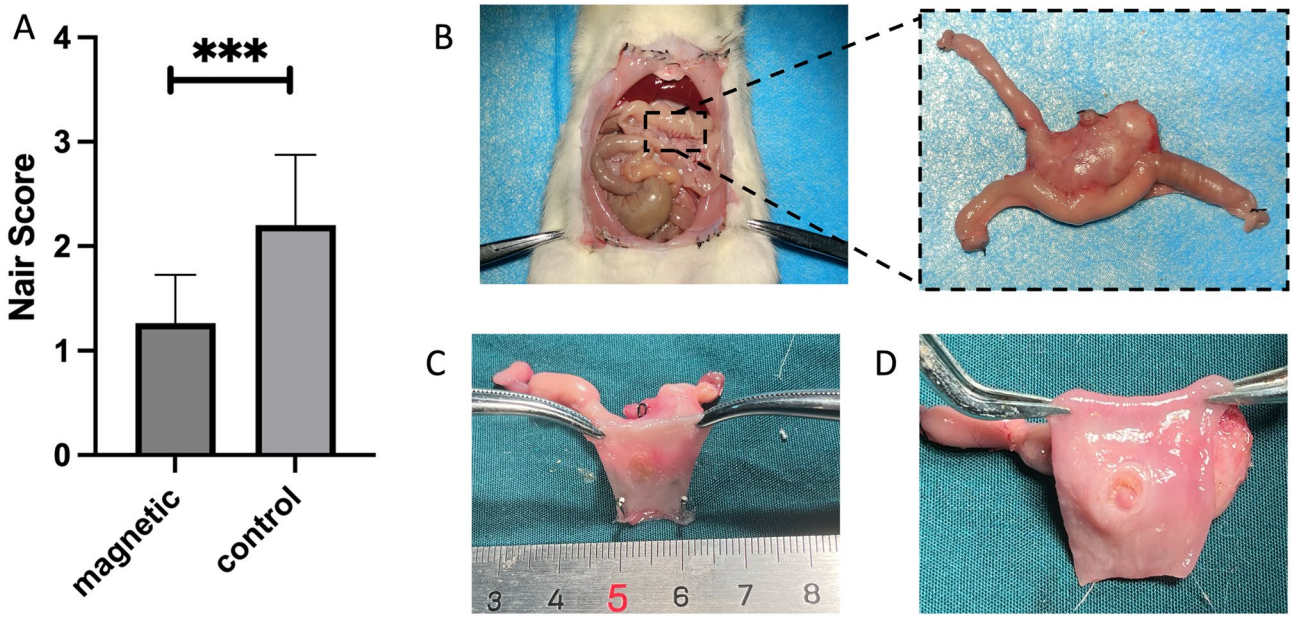

Fig. 3. The evaluation of abdominal adhesion. (**A**) The comparison of postoperative intra-abdominal adhesion scores shows that the magnamosis group has a significantly lower score than the suture anastomosis group; the Wilcoxon test was used (***$p < 0.001$). (**B**) Gross observation of intra-abdominal adhesions on postoperative day 5 in the magnamosis group shows only mild adhesions around the anastomotic site. (**C**,**D**) Observation of anastomotic site formation by cutting open the intestinal tube along the mesenteric edge of the jejunum reveals a smooth and well-formed anastomotic site.

Group	Scores														
	5d			6d			8d			10d			12d		
Magnetic	1	1	2	1	1	1	2	1	2	2	1	1	1	1	1
Control	2	3	1	2	3	2	3	1	3	2	2	2	2	2	3

Table 1. Postoperative abdominal adhesion score of rats. The degree of abdominal adhesion was evaluated after dissection of rats 5-12d postoperatively. In the magnetic anastomosis group, rats exhibited mild or localized moderate adhesions during postoperative days 5–12, which could be easily separated bluntly; 11 rats had an adhesion score of 1, and 4 rats had an adhesion score of 2. In contrast, the control group showed severe intra-abdominal adhesions that were difficult to separate bluntly and often required sharp dissection; 1 rat had an adhesion score of 1, 8 rats had an adhesion score of 2, and 5 rats had an adhesion score of 3.

The magnetic forces of the eight pairs of magnetic rings were measured and ranged from 0.88 to 2.42 N. The average maximum magnetic force was 1.33 N (Fig. 4A–C), which provided an effective pressure for the anastomosis to form at an appropriate time. Upon microscopic observation 48 h postoperatively, a patent anastomosis was successfully established in the magnamosis group. Tissue sectioning at 5 days postoperatively showed that the serosal surface of the magnamosis was smooth, with effective adhesion between the serosal layers. The original mucosal and muscular layers were inverted, with clear and paired layers, and no adhesions were observed in between. In contrast, the sutured anastomosis had a relatively smooth surface, with granulation tissue filling the gap between the gastric and intestinal walls. The original mucosal and muscular layers had disordered tissue layers (Figs. 5, 6). Comparison of the local granulation tissue areas in the two anastomosis groups revealed a significantly smaller average area in the magnamosis group ($2867 \pm 650\ \mu m^2$) than in the suture anastomosis group ($7792 \pm 4578\ \mu m^2$) ($P = 0.0388$) (Fig. 7).

Collagen density in the two anastomotic methods is similar

On Masson's staining, the collagen proteins appeared blue-purple. The blue-stained collagen protein regions within the granulation tissue area were selected, and their corresponding collagen synthesis densities were

Fig. 4. The magnetic ring used in surgery. (**A**) Physical representation of the anastomotic magnetic rings used during surgery. (**B**) A universal testing machine (Shenzhen Sansi Zongheng Technology Co., Ltd., Shenzhen, China) was used to measure the actual attraction force between the magnetic rings. (**C**) The mean magnetic force-distance curve shows a mean peak force of 1.33 N.

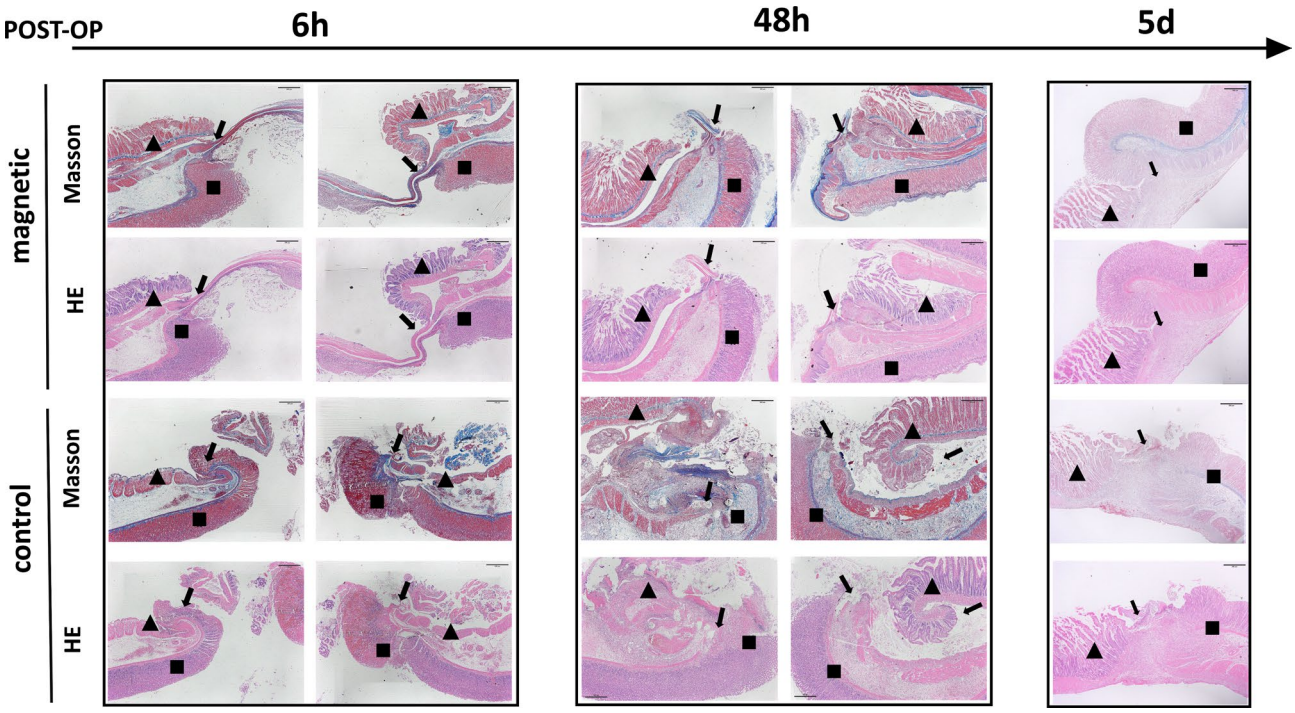

Fig. 5. Histopathological slice observations, with the square symbol marking the gastric side of the anastomosis, triangular symbol marking the jejunal side of the anastomosis, and black arrows indicating the anastomotic site. Scale bar = 20 μm. Hematoxylin and eosin (HE) staining, as well as Masson's trichrome staining six, 48 h, and 5 days postoperatively. Significant tissue compression was observed 6 h after magnamosis establishment, and tissue perforation occurred as early as 48 h postoperatively. The earliest time point at which tissue continuity was established was at postoperative day 5.

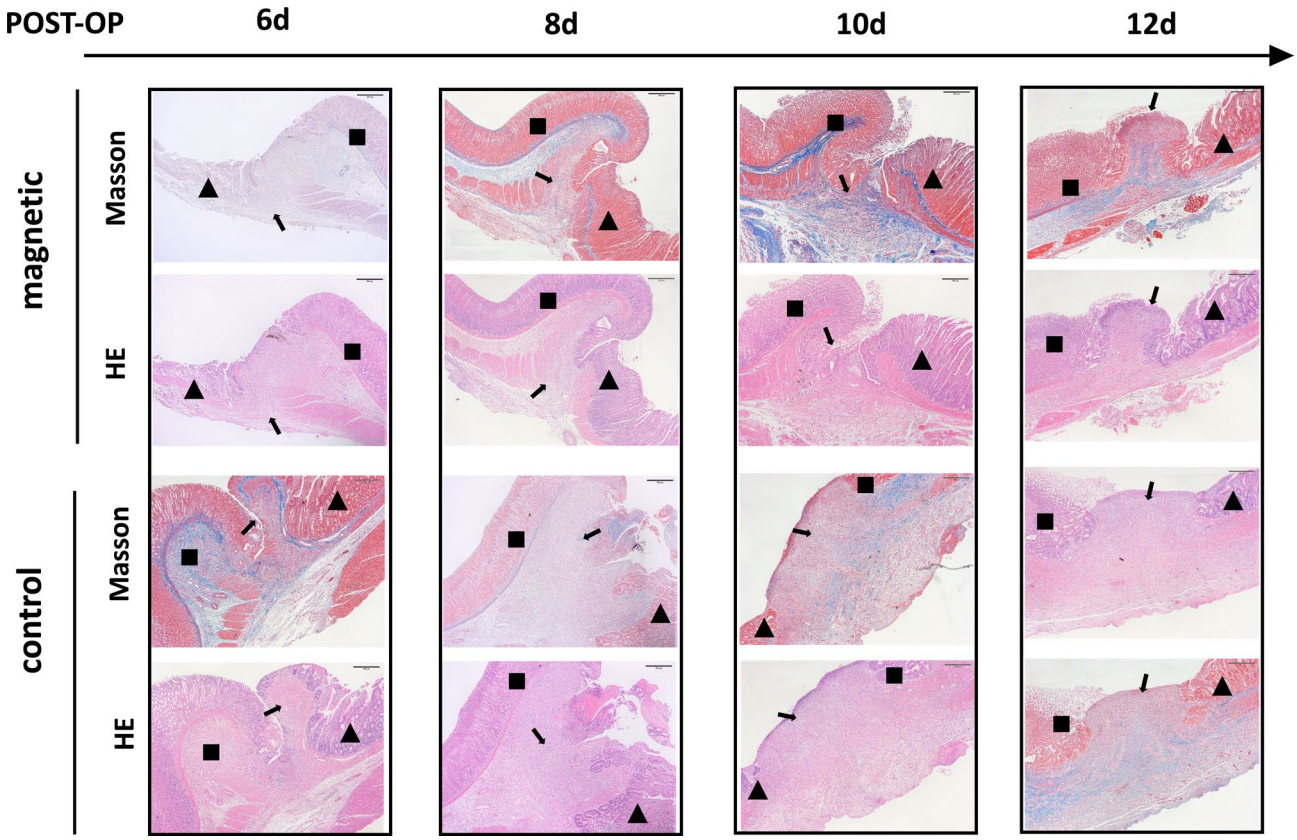

Fig. 6. Histopathological slice observations, with the square symbol marking the gastric side of the anastomosis, triangular symbol marking the jejunal side of the anastomosis, and black arrows indicating the anastomotic site. Scale bar = 20 μm. HE staining and Masson's trichrome staining 6, 8, 10, and 12 days postoperatively show the microscopic morphology of the tissue after the formation of the anastomosis. Tissue sectioning reveals that magnamosis resulted in a smooth serosal surface with well-adhered layers. The mucosal and muscular layers are inverted, forming clear and paired layers without adhesions. In contrast, the sutured anastomosis exhibits a relatively smooth surface, with granulation tissue filling the gap between gastric and jejunal walls. The original mucosal and muscular layers show disordered tissue layers.

calculated. The average density in the magnamosis group was 0.2896 ± 0.3045, whereas that in the suture anastomosis group was 0.1074 ± 0.0448. However, there was no significant difference between the two groups ($P = 0.3631$) (Fig. 8A,B). The local collagen density in the magnetic anastomosis group was slightly higher than that in the suture anastomosis group, but the difference was not statistically significant due to the limited sample size.

Magnamosis downregulates the expression of TGF-β1 and HIF-1α

In the localized area of magnamosis, where direct compression of the tissue edges occurred, and effective tissue adhesion healing took place, the expression of TGF-β1 and HIF-1α in fibroblasts of the submucosal layer of the gastrojejunal wall was analyzed. The comparison of the percentage of positively stained cells in the anastomotic tissues between the two anastomosis methods revealed that in the early stages of anastomosis formation (at 24 and 48 h postoperatively), both TGF-β1 and HIF-1α expression levels were lower in the magnamosis group than in the suture anastomosis group (Fig. 8C–H and Table 2).

Discussion

Poor healing at gastrointestinal anastomotic sites is a common and serious complication of gastrointestinal surgery that significantly affects early recovery and the long-term prognosis of patients[18]. Lowering the occurrence of the anastomotic healing impairment post-surgery and further developing new anastomosis techniques or devices to improve the healing process have long been hot topics in surgical research. Magnamosis is a novel method that utilizes attractive forces between magnets to establish compression and create anastomoses in tissues. This technique is relatively simple to perform and allows for rapid sutureless anastomosis[19]. Compared with sutured anastomosis, magnamosis applies unique tissue compression, leading to distinct pathological tissue healing processes associated with specific molecular mechanisms. In this study, gastrojejunal magnamosis was implemented, and the anastomoses in SD rats were sutured. The differences in granulation tissue proliferation at the anastomotic sites between the two anastomosis methods from a histopathological perspective were examined.

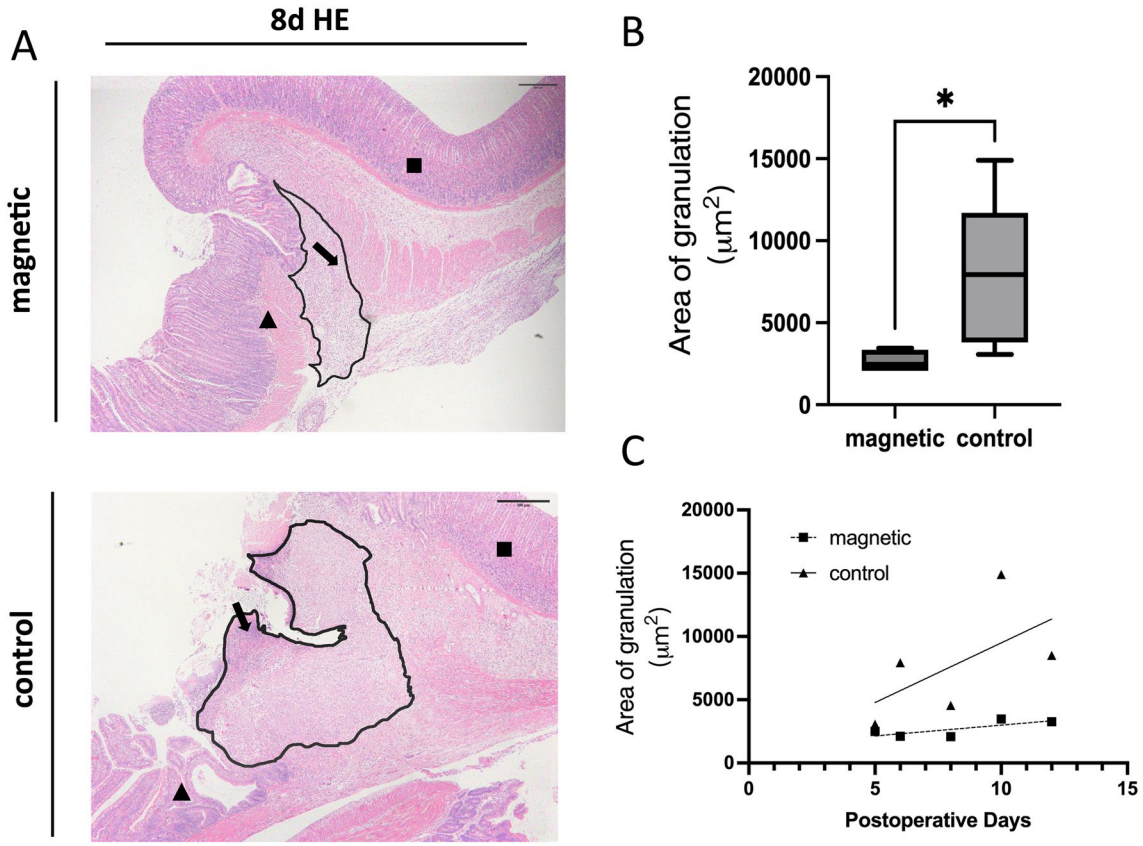

Fig. 7. Comparison of the local granulation tissue areas in the two anastomosis groups, with the square symbol marking the gastric side of the anastomosis, triangular symbol marking the jejunal side of the anastomosis, and black arrows indicating the anastomotic site. (**A**) Representative HE staining of tissue slices from the anastomotic site of both anastomosis methods on postoperative day 8. The granulation tissue area was measured and quantitatively compared using ImageJ. Scale bar = 200 μm. (**B**) Quantitative comparison of local granulation tissue area at the anastomotic site. The magnamosis group exhibits significantly less granulation tissue under the microscope than does the suture anastomosis group (*$p < 0.05$). (**C**) The scatter diagram shows the change in granulation tissue area over time, with linear fitting.

Additionally, the collagen synthesis density was quantitatively assessed, and the expression levels of collagen synthesis pathway-related growth factor TGF-β1 and the hypoxia-associated factor HIF-1α were measured.

The application of magnetic anastomosis technology in clinical practice has been widely developed, with reported surgical complications including[20] abdominal pain, abdominal discomfort, diarrhea, intestinal fistula, multiple bowel segments being clamped, bleeding, anastomotic stenosis, and intestinal obstruction. Currently, the magnetic anastomosis technology most commonly used in clinical trials is the placement of magnetic rings under endoscopy to establish an anastomosis[21]. This technique has been proven to be safe and feasible in the re-anastomosis of congenital esophageal atresia[19], biliary-intestinal anastomosis, and gastrointestinal anastomosis. Chopita et al.[22] were the first to propose using magnetic anastomosis technology to treat gastrointestinal obstruction, including 15 cases of malignant duodenal gastrointestinal obstruction, with 4 cases (30.76%) experiencing mild postoperative complications and no surgical deaths. Prospective clinical studies are needed to further verify the clinical application safety of magnetic anastomosis technology.

In animal experiments, we focused on the impact of postoperative anastomotic leakage, stenosis, and obstruction on animal survival. In this study, all rats survived postoperatively without fatal gastrointestinal complications. In the study by Yan et al.[23] one case of gastrointestinal obstruction occurred in the rat gastric magnetic anastomosis surgery, but the complication rate was lower compared to the control group. Considering long-term complications, Xu et al.'s study[17] mentioned one case each of long-term anastomotic stenosis in both the experimental group and the control group, which did not occur in this study.

The gross anatomical examination demonstrated that the anastomotic site appeared smooth and well-aligned, and fibrous tissue proliferation was not observed at the anastomotic site after 12 days in the magnamosis group. Many studies have been conducted on the feasibility of magnamosis using animal models. Similar to this study, Yan et al.[23] verified the feasibility of gastrojejunal magnetic anastomosis surgery by comparing the differences in surgical time, anastomotic burst pressure, and histopathological sections of the anastomosis in a rat gastrointestinal anastomosis model with two types of magnetic devices. In our study, suture anastomosis was used as a control group and a relatively in-depth investigation into the improvement of tissue healing was conducted while verifying the safety and feasibility of magnetic anastomosis surgery. Zhang et al.[24] proposed a "yan-zhang" staging

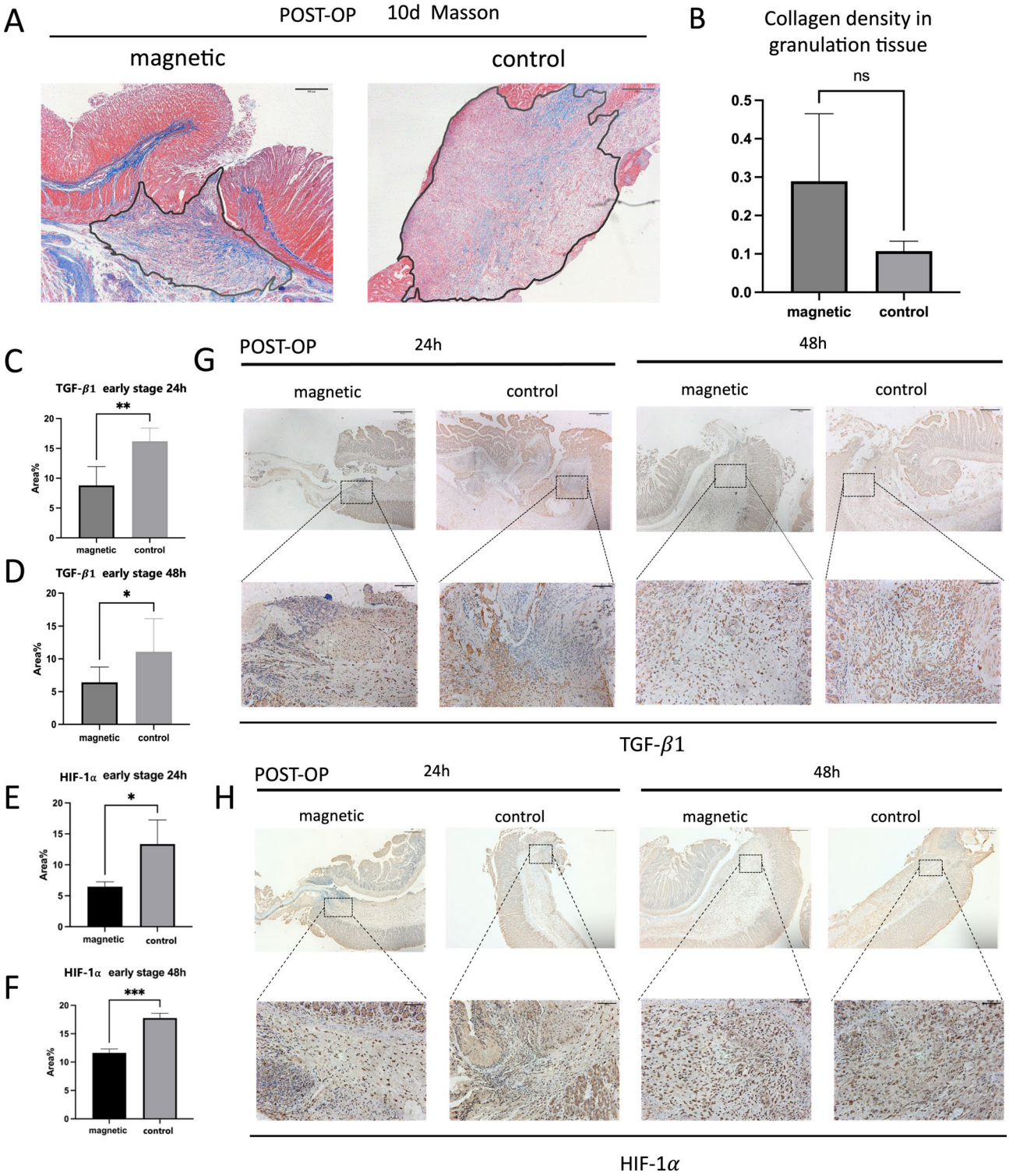

Fig. 8. Density of local collagen synthesis, as well as TGF-β1 and HIF-1α expression levels, at the anastomotic site, with the square symbol marking the gastric side of the anastomosis, triangular symbol marking the jejunal side of the anastomosis, and black arrows indicating the anastomotic site. (**A**) Representative Masson's trichrome staining of the anastomotic site on postoperative day 10. The density of collagen synthesis in granulation tissue was measured and quantitatively compared using Image J. Scale bar = 20 μm. (**B**) There was no statistically significant difference in the density of collagen synthesis (mean ± SD) in newly formed granulation tissue between the two anastomosis methods (ns, not significant); the local collagen density in the magnetic anastomosis group was slightly higher than that in the suture anastomosis group, but the difference was not statistically significant due to the limited sample size. (**C**–**H**) Immunohistochemical staining results at the edge of the compressed magnamosis and suture anastomosis incisions. (**C**–**F**) Percentage of positive cells (mean ± SD) expressing collagen synthesis-related molecules in the early phase after the establishment of the anastomotic site (within 48 h postoperatively) for TGF-β1 (**C**,**D**) and HIF-1α (**E**,**F**) expression levels. The magnamosis group showed significantly lower expression levels than did the suture anastomosis group (*$p < 0.05$, **$p < 0.01$, ***$p < 0.001$). (**G**,**H**) Immunohistochemical staining results at the edge of the anastomotic site on postoperative 24 and 48 h for both anastomosis methods. Scale bar = 20 μm; Scale bar in partially enlarged image = 200 μm.

Group		Positive cells area (%)		*P* value
		Magnetic	Control	
TGF-β1	24 h	8.79 ± 3.17	16.19 ± 2.21	0.0052
	48 h	6.43 ± 5.79	11.09 ± 5.50	0.0385
HIF-1α	24 h	6.48 ± 0.787	13.36 ± 3.90	0.0402
	48 h	11.65 ± 0.657	17.76 ± 0.80	0.0005

Table 2. Comparison of the proportion of positive cells (mean ± SD) in immunohistochemical staining of anastomosis, $P < 0.05$ indicating statistical significance.

system based on variations in anastomotic burst pressure in a rat gastrointestinal anastomosis model. According to this staging system, the anastomotic burst pressure remained moderate until 3 days postoperatively, when a burst pressure nadir occurred after magnetic detachment. As healing progressed, the anastomotic burst pressure gradually increased and reached its peak 21 days postoperatively. The histopathological findings from sequential samples of anastomotic tissues in their study indicated that the continuity of colonic end-to-end anastomosis following magnamosis was established 11 days postoperatively. Proliferative granulation tissue was observed under the microscope, and the tissue layers were well-apposed, which is consistent with the results obtained in our study. In a study by Xu et al.[17] the feasibility of end-to-end magnamosis of the esophagus was verified in a dog model. Long-term (6 months) therapeutic evaluation of the anastomotic site showed that the anastomosis site was smoother in the magnamosis group than in the sutured anastomosis group, with only a small amount of scar tissue observed in the sutured anastomosis group, consistent with the results of our study.

Comparing the microscopic granulation tissue areas of the two types of anastomotic sites, the magnamosis group exhibited a significantly smaller granulation tissue area than that in the sutured anastomosis group. However, when calculating the collagen synthesis density of the newly formed granulation tissue, there was no significant difference between the two types of anastomoses. This suggests that magnamosis can achieve anastomotic strength equivalent to sutured anastomosis but with less granulation tissue proliferation.

Fibroblasts are the most common cells in the connective tissue of the body and are responsible for the production, deposition, and integration of matrix proteins[25]. In the early stages of the inflammatory response, particularly during the proliferative phase (24–48 h after injury), the first batch of fibroblasts is recruited to the injury site. In an environment where macrophages secrete TGF-β, fibroblasts undergo phenotypic differentiation[6], along with the deposition of extracellular matrix, including collagen types I, III, and IV[2]. By the 4th–5th day of gastrojejunal tissue healing, fibroblasts become the primary cellular component of the healing site, with their recruitment primarily regulated by TGF-β1[9]. The study found that, at 24 and 48 h post-surgery, during the tissue healing and proliferative phase, the magnamosis group exhibited a lower percentage of TGF-β1-positive cells compared with the sutured anastomosis group, indicating that the local expression of TGF-β1 by fibroblasts in the magnamosis group was lower. These results suggest that magnamosis influences the process of collagen synthesis by regulating TGF-β1 expression. Specifically, it results in lower TGF-β1 expression during the healing and proliferative phases, leading to reduced fibroblast recruitment, weaker collagen synthesis, and, ultimately, a smoother anastomotic site with less granulation tissue proliferation.

Previous research has indicated that wound and tissue damage disrupt microcirculation, creating a hypoxic microenvironment that can activate the tissue healing process[26]. HIF-1 is a heterodimeric transcription factor and a primary regulator of tissue oxygen homeostasis[27]. This transcription factor remains inactive when oxygen is abundant but is activated under hypoxic conditions[7,28]. Yan Shi et al.[29] have shown that under hypoxic conditions, human bone marrow mesenchymal stem cells express HIF-1α, which, in turn, promotes the expression and secretion of TGF-β1. Additionally, Basu et al.[30] have confirmed that in chronic kidney fibrotic diseases caused by renal dysfunction, TGF-β1 promotes the translation of HIF-1α during the occurrence of renal fibrosis. The results of this study demonstrate that hypoxia caused by magnetic compression is milder in the anastomotic tissue than in acute trauma-induced hypoxia in sutured anastomoses. Within the early stages of anastomotic establishment (within 48 h postoperatively), the magnamosis group exhibited a lower percentage of HIF-1α-positive cells compared with the sutured anastomosis group. Differences in the degree of tissue hypoxia may affect the expression of TGF-β1 signaling, consequently leading to changes in granulation tissue proliferation and collagen synthesis. This study demonstrated that magnetic anastomosis can improve the healing of anastomotic tissues and cause changes in the expression levels of healing-related growth factors. This provides a new approach for the clinical development of new anastomosis methods and reduces anastomosis-related postoperative complications, promoting the widespread application of magnetic anastomosis in clinical practice. However, one limitation of this study is that it only identified downregulation of TGF-β1 and HIF-1α expression in magnetic anastomosis. The dynamic changes in tissue hypoxia levels in the anastomotic tissue and the specific interaction mechanisms between TGF-β1 and HIF-1α have not been extensively explored and require further investigation.

In conclusion, in the rat gastrojejunal anastomosis model, magnamosis led to improved tissue healing at the gastrojejunal anastomosis site, which was associated with the downregulated expression levels of TGF-β1 and HIF-1α.

Methods

Ethical considerations

The research protocol was approved by the Xi'an Jiaotong University Animal Experiment Ethics Committee (Ethical Review Approval Number: XJTUAE2020-70). This study was conducted in strict accordance with the guidelines of the Xi'an Jiaotong University Medical Center Guidelines for Care and Use of Laboratory Animals, with a focus on minimizing animal suffering and ensuring animal welfare. The principles of "3R" in animal experiments were strictly followed, making every effort to reduce the number of animals used while ensuring the achievement of the research objectives. This study is reported in accordance with ARRIVE guidelines (Animal Research: Reporting of In Vivo Experiments) 2.0.

Experimental animals

Forty-eight male Sprague–Dawley (SD) rats (200–300 g, aged ≤ 2 months) were obtained from the Xi'an Jiaotong University Medical School Experimental Animal Center. All animals were housed in individual cages in a Biosafety Level 2 (BSL-2) laboratory, with a room temperature of 20–25 °C, relative humidity of 30–70%, and a 12-h light/dark cycle. Food and water were provided ad libitum. Experimental animals were randomly divided into two groups based on the surgical procedure as follows: the gastrojejunal magnetic anastomosis group (experimental group, n = 24) and the sutured anastomosis group (control group, n = 24). The animals were acclimatized for 3 days before the start of the experiment under controlled conditions (23 °C, 12-h light–dark cycle, 50% humidity, and access to food and water). All surgeries were performed on a thermostatic rat dissection table.

Magnet design

Two neodymium-iron-boron (NdFeB, N45) ring magnets with an outer diameter of 6 mm, inner diameter of 4 mm, and thickness of 1 mm were selected for magnetic anastomosis of the rat stomach and intestine (Fig. 3A). The magnets were obtained from the Northwest Institute for Nonferrous Metal Research in Xi'an City, Shaanxi Province, China. N45 neodymium-iron-boron sintered alloy material was selected for magnet ring processing and was saturated with magnetization. The same batch of processed magnet rings was used for surgery. However, due to the manufacturing process, there were fluctuations in the actual magnetic force of the magnet rings. Therefore, the magnet rings were screened before use. The error in the magnetic force of the magnet rings has a negligible effect on healing.

Measurement of magnetic force-distance curve

The UTM6202 electronic universal testing machine (Shenzhen Sansi Zongheng Technology Co., Ltd., Shenzhen, China) (Fig. 3B) was used to measure the maximum attractive force of the magnets and the change in the magnetic force between the two magnets as the distance between them varied. A magnetic force-distance curve was generated based on these measurements.

Preoperative preparation

The experimental rats were subjected to 12 h fasting before surgery and were then anesthetized via intraperitoneal injection of pentobarbital solution. Subsequently, the rats were fixed on a temperature-controlled surgical table, their abdominal fur was shaved, and the skin was thoroughly disinfected with iodine solution (type III skin and mucous membrane disinfection) using sterile surgical instruments throughout the procedure. A midline abdominal incision, approximately 4 cm in length, was made, and access to the abdominal cavity was achieved through layered dissection.

Gastrojejunal magnetic anastomosis

The stomach and portion of the jejunum were exposed. Using 6-0 absorbable sutures (Shanghai Pudong Jinhuan Medical Supplies Co., Ltd., Shanghai, China), a purse-string suture was placed in the gastric fundus, followed by the creation of a 3–4 mm incision. A magnetic ring was inserted, and the purse-string suture was tightened to secure the knot. In the jejunum, a 3–4 mm longitudinal incision was made along the antimesenteric edge, approximately 10–15 cm from the ligament of Treitz, and another magnetic ring was inserted. This brought the two magnetic rings together, causing them to attract each other and form an anastomosis between the stomach and jejunum. The jejunal incision was sutured using 6-0 absorbable sutures (Fig. 9A–D).

Gastrojejunal suture anastomosis

A full-thickness incision, 3–4 mm in length, was made on the anterior wall of the stomach near the greater curvature in a vascular-free zone. Similarly, a 3–4 mm longitudinal incision was made on the jejunum of the rats, approximately 10–15 cm from the ligament of Treitz along the mesenteric edge. These two incisions were sutured using 6-0 absorbable sutures in an Albert–Lembert double-layer pattern (Fig. 9E–G).

The duration of the surgery was calculated from the commencement of gastrojejunal ostomy or the completion of anastomotic suturing using magnets and concluded at the same point. The durations of the two surgical techniques were then compared. After surgery, the anastomotic sites were reexamined for leakage and bleeding. The abdomen was closed layer-by-layer using 4-0 non-absorbable sutures. Local infiltration anesthesia with lidocaine was administered for pain relief, and penicillin was injected intramuscularly to prevent infection for 3 days postoperatively.

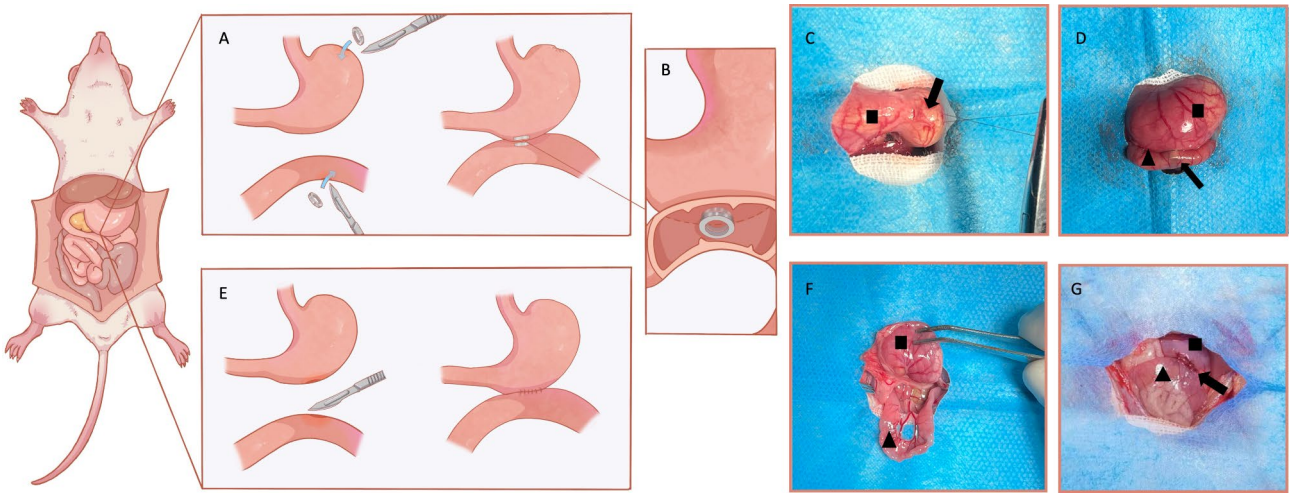

Fig. 9. Schematic illustration of gastric-jejunal anastomosis in Sprague–Dawley rats, with the square symbol marking the gastric side of the anastomosis, triangular symbol marking the jejunal side of the anastomosis, and black arrows indicating the anastomotic site. (**A**) Experimental group—Magnamosis. Magnetic rings were inserted through the gastric fundus and the mesenteric edge of the jejunum and adhered to the greater curvature side of the stomach. (**B**) In the post-anastomosis state, magnetic rings were observed on the mucosal surface of the jejunum. (**C**) In the gastric-jejunum magnamosis group, a purse-string suture was placed at the gastric fundus, and the magnet ring was inserted after the ostomy, as indicated by the arrow at the gastric fundus. (**D**) The location of the magnet ring inside the jejunum after gastric-jejunum magnetic anastomosis is marked by the black arrow, which represents the anastomotic site. (**E**) Control group—suture anastomosis: Equal-sized incisions were made on the greater curvature of the stomach and along the mesenteric edge of the jejunum, which were sutured together. (**F**) In the gastric-jejunum suture anastomosis group, the stomach and jejunum were exposed. (**G**) The black arrow in the image points to the anastomotic site upon completion of gastric-jejunum suture anastomosis.

Postoperative care

No special treatment was given to the abdominal wound after surgery; routine disinfection with type III iodine povidone was performed. Immediately after surgery, abdominal radiography was performed to assess the position of the magnets and coupling formation. The rats continued fasting for 12 h, after which their regular diet was resumed. During postoperative housing, 3–4 rats that underwent the same surgery were housed together. Daily monitoring of the animals' weights and abdominal radiographs was conducted to observe changes in magnet position until the magnets were naturally expelled from the body.

Anastomotic site sampling and adhesion scoring

According to the experimental groups, rats were euthanized at postoperative time points of 6 h, 24 h, 48 h, 5 d, 6 d, 8 d, 10 d, and 12 d, followed by the collection of anastomotic site samples. Mice were euthanized via intraperitoneal injection of an overdose of pentobarbital (500 mg/kg). During dissection, the anastomotic site was evaluated for its formation, the extent of inflammatory exudation, the presence of local ischemic necrosis, adhesions, anastomotic fistulas, anastomotic stenosis, and omental wrapping. This assessment followed the Nair five-grade scoring system (Table 3) to gauge the extent of intraabdominal adhesions, and photographs were taken for documentation. Circular tissue samples were collected 2–3 mm from the edge of the anastomosis, and the anastomotic tissue ring was cut longitudinally, fixed on foam boards, and immersed in a formaldehyde-based tissue fixative for subsequent pathological section staining.

Paraffin section processing and pathological observation

The intestinal segments containing the anastomotic site were embedded in paraffin, and 4-μm thick sections were cut at the anastomotic site. The sections were stained with hematoxylin, eosin, and Masson's trichrome. The tissue

Grade	Adhesion situation	Score
0	There is no adhesion at all	0
I	Very thin adhesion individually	1
II	Or two slight adhesions, glue related wide < 1 cm individually	2
III	Serious degrees of adhesion, two or more adhesion of first glue relatedly and widely > 1 cm	3
IV	The extensive one or the adhesion under the notch	4

Table 3. Nair five classification standard.

healing process, including anastomotic site continuity, granulation tissue area, and collagen synthesis density, was observed under a light microscope at 40× magnification. The Image J 2.9.0 software was used to process the section images, with a threshold of 0–80, to measure the granulation tissue area under the microscope. The collagen synthesis density in the granulation tissue was calculated using Masson staining as the ratio of the area of blue-stained collagen to the area of the granulation tissue.

TGF-β1 and HIF-1α immunohistochemical staining analysis

The sections were deparaffinized and rehydrated, and endogenous peroxidase activity was blocked with 3% H_2O_2. Next, the sections were subjected to antigen retrieval by immersion in a sodium citrate buffer (10 mmol/L, pH 6.0), followed by heat treatment for 3 min under saturated conditions. The sections were blocked with normal goat serum, followed by overnight incubation with primary antibodies (Wuhan Servicebio Technology Co., Ltd., Wuhan, China) at 4 °C. The sections were incubated with secondary antibodies at 37 °C the following day. The sections were then incubated with a third antibody, followed by diaminobenzidine development and counterstaining with hematoxylin. All the sections were independently observed by two pathologists using a light microscope [Olympus (Beijing) sales and service co., ltd., Beijing, China]. The Image J 2.9.0 software was used to process the images, with a threshold of 0–120, to measure the percentage of positive cells in three high-power fields for comparison.

Statistical methods

Data analysis was performed using the GraphPad Prism 9 (GraphPad Software, Boston, MA, USA) statistical software. For quantitative data obtained in the study, the two-sample independent *t*-test was employed for comparisons, with $P < 0.05$ considered statistically significant. Normally distributed data are presented as means. In assessing the abdominal adhesion scores following gastrojejunal anastomosis in the two groups, the Wilcoxon test was used, as the variables were discrete count data, with $P < 0.05$ indicating statistical significance.

Data availability

Data are available from the corresponding author on request.

Received: 13 December 2023; Accepted: 26 August 2024
Published online: 02 September 2024

References

1. Reischl, S., Wilhelm, D., Friess, H. & Neumann, P.-A. Innovative approaches for induction of gastrointestinal anastomotic healing: An update on experimental and clinical aspects. *Langenbecks Arch. Surg.* **406**, 971–980 (2021).
2. Thompson, S. K., Chang, E. Y. & Jobe, B. A. Clinical review: Healing in gastrointestinal anastomoses, Part I. *Microsurgery* **26**, 131–136 (2006).
3. Enestvedt, C. K., Thompson, S. K., Chang, E. Y. & Jobe, B. A. Clinical review: Healing in gastrointestinal anastomoses, Part II. *Microsurgery* **26**, 137–143 (2006).
4. Tracy, L. E., Minasian, R. A. & Caterson, E. J. Extracellular matrix and dermal fibroblast function in the healing wound. *Adv. Wound Care* **5**, 119–136 (2016).
5. Lichtman, M. K., Otero-Vinas, M. & Falanga, V. Transforming growth factor beta (TGF-β) isoforms in wound healing and fibrosis. *Wound Repair Regen.* **24**, 215–222 (2016).
6. Talbott, H. E., Mascharak, S., Griffin, M., Wan, D. C. & Longaker, M. T. Wound healing, fibroblast heterogeneity, and fibrosis. *Cell Stem Cell* **29**, 1161–1180 (2022).
7. Eltzschig, H. K. & Carmeliet, P. Hypoxia and inflammation. *N. Engl. J. Med.* **364**, 656–665 (2011).
8. Yoshimoto, S., Tanaka, F., Morita, H., Hiraki, A. & Hashimoto, S. Hypoxia-induced HIF-1α and ZEB1 are critical for the malignant transformation of ameloblastoma via TGF-β-dependent EMT. *Cancer Med.* **8**, 7822–7832 (2019).
9. Rijcken, E., Sachs, L., Fuchs, T., Spiegel, H.-U. & Neumann, P.-A. Growth factors and gastrointestinal anastomotic healing. *J. Surg. Res.* **187**, 202–210 (2014).
10. Pichakron, K. O. *et al.* Magnamosis II: Magnetic compression anastomosis for minimally invasive gastrojejunostomy and jejuno-jejunostomy. *J. Am. Coll. Surg.* **212**, 42–49 (2011).
11. Zhang, X. *et al.* Definition and application of magnetic compression anastomosis. *Chin. Sci. Bull.* **65**, 1173–1180 (2020).
12. Jamshidi, R., Stephenson, J. T., Clay, J. G., Pichakron, K. O. & Harrison, M. R. Magnamosis: Magnetic compression anastomosis with comparison to suture and staple techniques. *J. Pediatr. Surg.* **44**, 222–228 (2009).
13. Gonzales, K. D. *et al.* Magnamosis III: Delivery of a magnetic compression anastomosis device using minimally invasive endoscopic techniques. *J. Pediatr. Surg.* **47**, 1291–1295 (2012).
14. Wall, J. *et al.* MAGNAMOSIS IV: Magnetic compression anastomosis for minimally invasive colorectal surgery. *Endoscopy* **45**, 643–648 (2013).
15. Du, X., Fan, C., Zhang, H. & Lu, J. Application value of magnetic compression anastomosis in digestive tract reconstruction. *Zhonghua Wei Chang Wai Ke Za Zhi* **17**, 512–515 (2014).
16. Scientific Committee of the First International Conference of Magnetic Surgery, Lv, Y. & Shi, Y. Xi'an consensus on magnetic surgery. *Hepatobiliary Surg. Nutr* **8**, 177–178 (2019).
17. Xu, X.-H., Lv, Y., Liu, S.-Q., Cui, X.-H. & Suo, R.-Y. Esophageal magnetic compression anastomosis in dogs. *World J. Gastroenterol.* **28**, 5313–5323 (2022).
18. Marrache, M. K. *et al.* Endoscopic gastrointestinal anastomosis: A review of established techniques. *Gastrointest. Endosc.* **93**, 34–46 (2021).
19. Krishnan, N. *et al.* Role of magnetic compression anastomosis in long-gap esophageal atresia: A systematic review. *J. Laparoendosc. Adv. Surg. Tech. A* **33**, 1223–1230. https://doi.org/10.1089/lap.2023.0295 (2023).
20. Kamada, T. *et al.* New technique for magnetic compression anastomosis without incision for gastrointestinal obstruction. *J. Am. Coll. Surg.* **232**, 170-177e2 (2021).
21. Zhang, G., Liang, Z., Zhao, G. & Zhang, S. Endoscopic application of magnetic compression anastomosis: A review. *J. Gastroenterol. Hepatol.* https://doi.org/10.1111/jgh.16574 (2024).
22. Chopita, N. *et al.* Endoscopic gastroenteric anastomosis using magnets. *Endoscopy* **37**, 313–317 (2005).
23. An, Y. *et al.* Gastrojejunal anastomosis in rats using the magnetic compression technique. *Sci. Rep.* **8**, 11620 (2018).

24. Zhang, M. *et al.* Establishment of Yan-Zhang's staging of digestive tract magnetic compression anastomosis in a rat model. *Sci. Rep.* **12**, 12445 (2022).
25. Lynch, M. D. & Watt, F. M. Fibroblast heterogeneity: Implications for human disease. *J. Clin. Investig.* **128**, 26–35 (2018).
26. Ahluwalia, A. & Tarnawski, A. S. Critical role of hypoxia sensor—HIF-1α in VEGF gene activation. Implications for angiogenesis and tissue injury healing. *Curr. Med. Chem.* **19**, 90–97 (2012).
27. Hong, W. X. *et al.* The role of hypoxia-inducible factor in wound healing. *Adv. Wound Care* **3**, 390–399 (2014).
28. Ciarlillo, D., Celeste, C., Carmeliet, P., Boerboom, D. & Theoret, C. A hypoxia response element in the Vegfa promoter is required for basal Vegfa expression in skin and for optimal granulation tissue formation during wound healing in mice. *PLoS One* **12**, e0180586 (2017).
29. Shi, Y. *et al.* Bone marrow mesenchymal stem cells facilitate diabetic wound healing through the restoration of epidermal cell autophagy via the HIF-1α/TGF-β1/SMAD pathway. *Stem Cell Res. Ther.* **13**, 314 (2022).
30. Basu, R. K. *et al.* Interdependence of HIF-1α and TGF-β/Smad3 signaling in normoxic and hypoxic renal epithelial cell collagen expression. *Am. J. Physiol. Renal Physiol.* **300**, F898–F905 (2011).

Acknowledgements

We are grateful to the staff at the National Local Joint Engineering Research Center for Precision Surgery and Regenerative Medicine for their excellent support this research.

Author contributions

T. R. W.: Investigation (lead); Methodology (equal); Writing—original draft (lead); Writing—review and editing (supporting). Y. H. L.: Investigation (supporting); Methodology (supporting); Writing—review and editing (equal). C. A. Y.: Investigation (supporting); Writing—original draft (supporting); Writing—review and editing (supporting). X. R. L.: Investigation (supporting); Writing—original draft (supporting); Writing—review and editing (supporting). Y. X. W.: Investigation (supporting); Methodology (supporting); Writing—original draft (supporting). Z. X. Z.: Investigation (supporting); Writing—review and editing (supporting). H. Z. X.: Investigation (supporting); Modification (supporting). R. J. L.: Modification (lead). M. Y. W.: Investigation (supporting). Z. Z. W.: Investigation (supporting). C. Z.: Investigation (supporting). Y. L.: Funding acquisition (equal); Resources (equal). Y. Z.: Funding acquisition (equal); Resources (equal); Supervision (lead); Writing—review and editing (lead).

Funding

This study was funded by Wu Jieping Medical Foundation research project (No. 202309184860), Innovation Training Program for Undergraduate of Xi'an Jiaotong University (No. S202310698452), Key Research and Development Projects of Shaanxi Province (No. 2019SF-014), Bethune Charitable Foundation (No. HZB-20181119-070), Shaanxi Provincial Health Research Foundation (No. 2018D056), Crosswise project of The First Affiliated Hospital of Xi'an Jiaotong University (No. HX201739), The basic scientific research in colleges and universities (No. xzd012020026), New Medical Technology Project of Xi'an Jiaotong University (No. XJLS-2019-048), New Medical Technology Project of The First Affiliated Hospital of Xi'an Jiaotong University (No. XJYFY-2019W3).

Competing interests

The authors declare no competing interests.

Additional information

Correspondence and requests for materials should be addressed to Y.L. or Y.Z.